Acta Physiologica Sinica, April 25, 2009, 61 (2): 185-193
http://www.actaps.com.cn

Research Paper

Mobilization of bone marrow-derived Nkx2-5$^+$ cardiac progenitor cells under condition of acute myocardial ischemia

DONG Hong-Yan[1,**], XU Zhi-Wei[2,**], ZHANG Zhong-Ming[2,*], YU Hong-Li[1], XU Xia-Hong[1]

[1]Center of Neurobiological Research; [2]Department of Cardiothoracic Surgery of Affiliated Hospital, Xuzhou Medical College, Xuzhou 221002, China

Abstract: The present study aimed to observe the morphological distribution of bone marrow (BM)-derived Nkx2-5$^+$ cardiac progenitor cells (CPCs) in bone marrow niche and evaluate the effect of acute myocardial ischemia (AMI) on the mobilizion of BM-derived Nkx2-5$^+$ CPCs. Animal models of BALB/c mouse AMI, cerebral and hind-limb ischemia were established. Nanogold labeling method, immunofluorescence and Western blot were used to identify the distribution of BM-derived Nkx2-5$^+$ CPCs and the expressions of Nkx2-5 protein in peripheral blood and BM after AMI. Meanwhile, in different ischemia organ models and after AMD3100 (SDF-1/CXCR4 antagonist) pretreatment in AMI model, Nkx2-5 protein expressions in peripheral blood were also assayed. Nkx2-5$^+$ CPCs were found to locate in cavitas medullaris. The percentage of Nkx2-5$^+$ CPCs in blood increased immediately after AMI. Nkx2-5 protein expression in peripheral blood was also upregulated at the timepoint of 24 h post-AMI (P<0.01) and kept stable without further enhancement from day 1 to day 7 post-AMI. In BM, Nkx2-5 protein expression was upregulated immediately after AMI and downregulated afterwards (P<0.01). After AMD3100 pretreatment in AMI group, Nkx2-5 protein expression was significantly inhibited in peripheral blood (P<0.05). In cerebral and hind-limb ischemia models, Nkx2-5 protein expressions were significantly lower than that in AMI group (P<0.01), but with no significant difference to control group. These results suggest that Nkx2-5$^+$ CPCs are physiologically resident in BM and AMI initiates mobilization of BM-derived Nkx2-5$^+$ CPCs in a predominant organ-specific manner. In the procedure of mobilization, SDF-1 may play a critical role in a chemoattracted manner.

Key words: cardiac progenitor cells; bone marrow; Nkx2-5; mobilization; myocardial ischemia

急性心肌缺血对骨髓 Nkx2-5$^+$ 心脏祖细胞的动员作用

董红燕[1,**]，徐志伟[2,**]，张中明[2,*]，于红丽[1]，徐夏红[1]

徐州医学院[1] 神经生物学研究中心；[2] 附属医院胸心外科，徐州 221002

摘 要：骨髓源性 Nkx2-5$^+$ 心脏祖细胞(bone marrow-derived Nkx2-5$^+$ cardiac progenitor cells)具有高度特异性分化为心肌细胞的潜能，在病理状态下可能参与内源性心肌修复。但在器官缺血、特别在急性心肌缺血病理状态下，该细胞如何被动员的机制尚不清楚。本研究在观察 Nkx2-5$^+$ 心脏祖细胞在骨髓中分布特征的基础上，分析急性心肌缺血对骨髓源性 Nkx2-5$^+$ 心脏祖细胞的动员作用，探讨其细胞动员的可能机制。分别建立小鼠急性心肌缺血及脑、后肢急性缺血动物模型。采用纳米金 - 银免疫标记透射电镜、免疫荧光标记及分子生物学等检测方法，观察骨髓 Nkx2-5$^+$ 心肌祖细胞的定位及其形态学特征；检测急性心肌缺血后外周血 Nkx2-5$^+$ 细胞比例变化、缺血不同时段骨髓及外周血中 Nkx2-5 蛋白表达的变化；比较不同器官缺血对 Nkx2-5$^+$ 心脏祖细胞的动员作用；应用 SDF-1/CXCR4 通路特异性阻断剂 AMD3100，分析 SDF-1 在急性心肌缺血后对 Nkx2-5$^+$ 心脏祖细胞动员作用的影响。结果显示：Nkx2-5$^+$ 心脏祖细胞呈散在分布于骨髓血窦旁。与对照组相比，急性心肌缺血后，外周血 Nkx2-5$^+$ 心脏祖细胞比例显著增加(P<0.01)。心肌缺血早期(1 d)，外周血 Nkx2-5 蛋白表达显著增加(P<0.01)，并可持续 7 d；而此间，骨髓中 Nkx2-5 蛋白表达立即升高，随后则降低。应用 AMD3100 阻断剂后，心肌缺血组外周血 Nkx2-5 蛋白表达受到明显抑制(P<0.05)。脑、后肢缺血后，外周血 Nkx2-5 蛋白表达显著少于急性心肌缺血组(P<0.01)，而与对照组相比无显著差异。上

Received 2008-12-03 Accepted 2009-02-19

This work was supported by Natural Science Foundation of Education Department of Jiangsu Province, China (No. 05KJD310235).

[**]These authors contributed equally to this work.

[*]Corresponding author. Tel: +86-516-85802033; E-mail: zhang_zhongming@yahoo.com.cn

述结果提示，生理状态下，骨髓中存在 Nkx2-5$^+$ 心脏祖细胞亚群；急性心肌缺血对骨髓 Nkx2-5$^+$ 心脏祖细胞具有显著的动员作用，且该动员作用具有显著的器官特异性，SDF-1/CXCR4 通路在该动员作用中发挥了重要的趋化作用。

关键词：心脏祖细胞；骨髓；Nkx2-5；动员；心肌缺血
中图分类号：R542.2

The regenerative capacity of cardiomyocyte is poor so that the heart itself can not repair serious injury and recover function by self-proliferation. Numerous basic studies were performed using a variety of cell types with the hope of improving myocardial performance. The studies on adult mammalian bone marrow (BM) mesenchymal stem cells (MSCs) have given rise to the upsurge of experiments and early-stage clinical trials to regenerate infarcted myocardium[1-5]. It is undoubted that BM could be a convenient source of autogeneic cell seeds without immunological rejection and available in large quantities for transplantation, thus, this solution represents a promising method.

However, many recent reports that are mainly concerned about the efficacy and safety of MSCs-based myocardial regeneration hold skeptical views to open an academic debate[6,7]. Because the detailed mechanisms that MSCs participate in myocardial regeneration remain highly controversial, altered interest to identify specific BM-derived cellular subset(s) for cardiomyocyte regeneration has been evoked extensively.

A recent study has revealed that BM contains not only haemopoietic stem cells (HSCs) and MSCs, but also a crowd of differentiated tissue-committed stem cells (TCSCs)[8]. TCSCs population maintains a high regenerative capacity of terminally differentiated organs both under basal condition and following local tissue injury. For instance, after the onset of myocardial ischemia, one of the TCSCs marked with Nkx2-5, GATA-4 and MEF-2C, also known as BM-derived cardiac progenitor cells (BM-derived CPCs), will be thereby mobilized into the peripheral blood circulation, via terminal homing to the ischemic myocardia, to initiate endogenous cardiomyocyte regeneration[9,10].

Nevertheless, the morphological evidence of Nkx2-5$^+$ CPCs residing in BM niche and the detailed mechanism of BM-derived CPCs mobilization, specially, the dynamic variation of Nkx2-5$^+$ CPCs in BM after acute myocardial ischemia (AMI), remain uncertain.

In this study, we set Nkx2-5, one of the pivotal factors of cardiomyogenesis, as the key marker, firstly, to observe the morphological distribution of BM-derived Nkx2-5$^+$ CPCs in BM niche, and secondly, to evaluate the effects of AMI on the mobilizion of BM-derived Nkx2-5$^+$ CPCs. Meanwhile, we intended to reveal the impacts of ischemia in different organs, besides the heart, on mobilizing BM-derived Nkx2-5$^+$ CPCs.

1 MATERIALS AND METHODS

1.1 *Animals*

BALB/c mice, 4 to 6 weeks old and weighing 16-25 g, were obtained from Experimental Animal Centre of Xuzhou Medical College. The animal studies were approved by the Animal Care and Use Committee of the Xuzhou Medical College. All animals received humane care in compliance with the Guideline for Care and Use of Laboratory Animals published by Jiangsu Province, China.

1.2 *Animal models*

Myocardial ischemia models were established by using sequential Isoprenaline (ISO) (Shanghai Harvest Pharmaceutical Co., Ltd. China) injection[11]. Briefly, high dose of ISO (10 mg/kg) was intraperitoneally injected once daily for 3 d with a 24-hour interval. As a negative control, ISO was replaced by 0.9% normal saline. An individual electrocardiogram was recorded once daily after ISO administration, and an ST-segment-elevation was considered as qualified model for further study. After total three days of ISO administration, under basal anesthesia induced by intraperitoneal injection of 2% Carbrital (40 mg/kg), animal hearts were harvested, embedded in paraffin, sliced into 5 μm sections and stained with Hematoxylin-Eosin for histologic assay.

To establish BALB/c mouse cerebral ischemia model, the animal anesthesia was initially induced by intraperitoneal injection of 2% Carbrital (40 mg/kg), and maintained by inhalation of 1.5% Halothane in 100% O_2 via face masks. The animal spontaneous breath was kept. With an inserted rectal probe, the body temperature was strictly controlled at 37 ºC during the procedure until the animals were placed in incubators. A midline cervical incision was made, taking care not to damage the vagus nerve, bilateral common carotid arteries were exposed and isolated using 4/0 silk suture line and the animals were allowed to stabilize for 5 min. The common carotid arteries were occluded using

microaneurysm clips applied bilaterally for exactly 17 min based on Horsburgh's method[12]. After completing vessels occlusion, the clips were removed and blood flow through the arteries was confirmed before the incision was closed. The animals were placed in an incubator and allowed to recover for at least 2 h and then returned to the animal housing.

For mouse hind-limb ischemia model, the tourniquets were employed to occlude femoral arteries of dual hind-limbs for 4 h to create limb ischemia under inhaled anesthesia of 1.5% Halothane. When skin thanatosis and functional disorder of involved limbs appeared, a successful animal model was confirmed.

1.3 *Experimental procedures*

The animal models presented above were divided into 7 groups (6 BALB/c mice for each group). Control group, normal mice without any treatment. Myocardial ischemia 0 d group (MI-0 d group), immediately after three days of sequential ISO injection, the heart and peripheral venous blood and BM samples were obtained. Myocardial ischemia 1d group (MI-1 d group), 24 h after sequential ISO injection, both blood and BM samples were obtained. Myocardial ischemia 7 d group (MI-7 d group), 7 d after sequential ISO injection, both blood and BM samples were obtained. AMD3100 pretreated group (AMD group), 10 mg/kg AMD3100 (an SDF-1/CXCR4 antagonist, Sigma, USA) was injected intraperitoneally 15 min prior to ISO administration, and immediately after completing the third time of ISO and AMD3100 injections, peripheral blood sample was obtained. Limb ischemic group (LI group), 48 h after limb ischemia, peripheral blood sample was harvested. Cerebral ischemic group (CI group), 48 h after cerebral ischemia, peripheral blood sample was harvested.

In all animal groups, peripheral blood was harvested from the animal's orbital plexus under inhaled anesthesia of 1.5% Halothane[13]. Femurs and shinbones were flushed with phosphate-buffered saline (PBS) to obtain BM sample. Mononuclear cells derived from blood and BM were isolated by density gradient centrifugation. In brief, the cells were washed three times with ice-cold PBS and separated by spallation buffer (containing 3-morpholino propanesulfonic acid 50 mmol/L, dithiothreitol 0.2 mmol/L, KCl 100 mmol/L, $MgCl_2$ 0.5 mmol/L, Na_3VO_4 10 mmol/L, EDTA 0.1mmol/L, ethylene glycol tetraacetate 1 mmol/L, saccharin 0.32 mol/L, leupeptin 5 μg/mL, pepstatin A 5 μg/mL, aprotinin 5 μg/mL, phenylmethyl sulfonylfluoride 0.1 mmol/L, benzamidine 0.1 mmol/L, NP-4 0.1%, pH 7.4) (Westang, Shanghai, China), and then centrifugalized at 12 000 *g* for 5 min at 4 ºC. The supernatant was used for further analysis.

1.3.1 *Morphological observation of BM-derived Nkx2-5$^+$ CPCs*

In control group, two animals' shinbones were obtained under inhaled anesthesia of 1.5% Halothane, and decalcification of the bones was performed based on the method described by Yu *et al*.[14]. Frozen longitudinal sections (70 μm) of decalcificated shinbones were made, which were immersed in 5% bovine serum albumin (BSA) for 1 h at room temperature for blocking non-special antigen. After being rinsed with PBS three times, the sections were incubated with goat-anti mouse Nkx2-5 polyclonal antibody (Santa Cruz, USA, 1:200) at 4 ºC for 48 h. Afterwards, the Nanogold-labeled secondary anti-goat IgG antibody (Nanoprobes, NY, USA, 1:100) was incubated with the sections for 60 min. As a negative control, the primary antibody was replaced by a non-immune serum. After being rinsed with PBS three times, the sections were initially fixed in 3% glutaraldehyde, postfixed in 1% osmium tetroxide and then enhanced with a silver acetate solution (Nanoprobes, NY, USA) for 7 min under protection from light at room temperature. After intensification, the sections were embedded in epoxy resin. Ultrathin sections cut horizontally were prepared. The sections were doubly stained by uranyl acetate and lead citrate. The ultrastructure of Nanogold positive CPCs was observed under H-600 transmission electron microscope (Hitachi Inc., Tokyo, Japan).

1.3.2 *Immunofluorescence for BM-derived Nkx2-5$^+$ CPCs*

Mice shinbones from control group were dehydrated and embedded in paraffin, and sequentially longitudinal sections (5 μm) were prepared. The deparaffinaged sections were immersed in citrate buffer for antigen recovery, and then immersed in 5% BSA for 1 h at room temperature for non-special antigen blocking. After that, the sections were incubated with goat-anti mouse Nkx2-5 polyclonal antibody (Santa Cruz, USA, 1:200) at 4 ºC overnight. The second rabbit anti-goat tetramethyl rhodamine isothiocyanate (TRITC)-conjugated antibody (Zhongshan Biology Company, Beijing, China, 1:50) was then incubated with the sections for 2 h under protection from light. As a negative control, the primary antibody was replaced by a non-immune serum. After being rinsed with PBS three times, the sections were immersed with buffer bicarbonate (pH=9.5) and observed by fluorescence microscope (Olympus Company, Japan). The photographs were taken under fluorescence and visible light fields, respectively. The loca-

tions of fluorescence positive CPCs were confirmed by overlapping two kinds of photographs taken from the same sample.

1.3.3 *Flow cytometry analysis*

For comparing the percentages of BM-derived Nkx2-5$^+$ CPCs in peripheral blood before and after AMI, the mononuclear cells derived from peripheral blood in control and MI-0 d groups were incubated with goat anti-mouse Nkx2-5 polyclonal antibody (Santa Cruz, USA, 1:200) at 4 ℃ for 1 h. The negative control was incubated with PBS. After brief washing, the cellular density was adjusted to 1×10^6-1×10^7/mL. The cells were incubated with rabbit anti-goat IgG conjugated with TRITC (Zhongshan, Beijing, China, 1:100) for 30 min at 4 ℃, and then the cells were fixed by 0.5% formaldehyde and analyzed by flow cytometry (FACS, Calibu, Becton Bickinson Company, USA).

1.3.4 *Western blot*

The supernatant prepared from both blood and BM samples in all groups was quantified for protein concentration by Lowry's method. Expression of Nkx2-5 protein level was assayed by immunoblotting.

Briefly, 50 μg protein was electrophoresed on 10% sodium dodecyl sulfate polyacrylamide gel and then transferred to a polyvinylidene difluoride membrane (Bio-Rad, Hercules, CA,USA) (pore size 0.45 μm) using an electroblotting apparatus (Bio-Rad, USA). Afterwards, the membrane was incubated with tris-buffered saline (TBS) containing 5% non-fat dry milk for 3 h at room temperature and then incubated with goat-anti Nkx2-5 polyclonal antibody (Santa Cruz, USA, 1:200) at 4 ℃ overnight. The membrane was washed with TBS for 10 min three times and incubated with alkaline phosphatase-labeled anti-goat IgG antibody (Zhongshan, Beijing, China, 1:500) for 2 h at room temperature, and then colorized with nitro blue tetrazolium and 5-bromo-4-chloro-3-indolyl phosphate (NBT/BCIP). The image bands were scanned by the image analyzer (UVP Inc., USA) and semi-quantitatively analyzed by Image J software (Image J v1.37. Wayne Rasband, USA).

1.4 *Statistical analysis*

Values were presented as mean±SD, and significance was determined by the one-way ANOVA. *P* value less than 0.05 was considered statistically significant.

2 RESULTS

2.1 Histological study

After sequential ISO injections, histological observation showed the disordered arrangement of cardiomyocytes, cellular degeneration and inflammatory cells infiltration. The fragmented cardiomyocytes with focal myocardial necrosis were also detectable (Fig. 1).

2.2 Ultrastructure characteristics of BM-derived Nkx2-5$^+$ CPCs

Morphological observation revealed that Nanogold positive CPCs existed in control group. The Nanogold positive CPCs showed a spindle or irregular appearance with larger volume, and some Nanogold particles with high electron density were found to distribute sporadically in cytoplasm. The transmission electron microscope pictures have been shown previously[14] and omitted here.

2.3 Location of Nkx2-5$^+$ CPCs in BM

In the shinbone longitudinal sections, our observation showed that a single or grouped red fluorescence (550 nm) was located in the cavitas medullaris, in which the volume of the cells emitting red fluorescence was larger than the surrounding osteoblasts. And also, the fluorescence positive CPCs were adjacent to the blood sinus inside cavitas medullaris (Fig. 2).

2.4 Flow cytometry determination

The flow cytometry determination showed that the percentage of BM-derived Nkx2-5$^+$ CPCs in peripheral blood mononuclear cells increased immediately after AMI. The percentage of Nkx2.5$^+$ cells in MI-0 d group was significantly higher than that in control group (8.02%±1.68% *vs* 2.33%±1.18%, $P<0.01$) (Fig. 3).

2.5 Expressions of Nkx2-5 protein in peripheral blood and BM

Expressions of Nkx2-5 protein in peripheral blood in MI-0, 1, 7 d groups were significantly higher than that in control group ($P<0.01$). In comparison with that in MI-0 d group, the levels of Nkx2-5 protein expression in MI-1, 7 d groups increased significantly ($P<0.05$), but there was no statistical significance between MI-1d and MI-7 d groups ($P>0.05$) (Fig. 4*A*). In BM, the expression of Nkx2-5 protein increased remarkably in MI-0 d group compared with that in control group ($P<0.05$). However, in MI-1, 7 d groups, the expressions of Nkx2-5 protein were significantly lower than that in MI-0 d group ($P<0.01$) (Fig. 4*B*). After AMD3100 administration, in peripheral blood, the expression of Nkx2-5 protein decreased significantly, compared with that in MI-0 d group ($P<0.05$). And there was no statistical significance between control and AMD group (Fig. 4*C*). The change trend of Nkx2-5 protein expression pre- and post-AMI in peripheral blood and BM was illustrated in Fig. 4*D*. Nkx2-5 protein expression in blood (solid line) was upregulated immediately after AMI

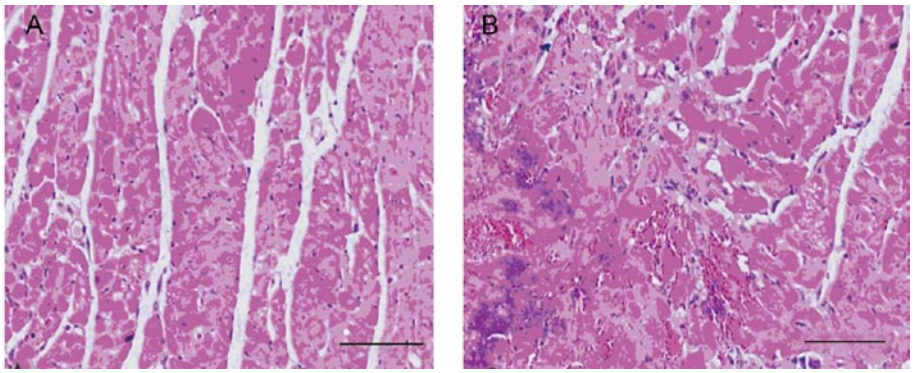

Fig. 1. Histological observation of ischemic myocardium. *A*: The myocardium from control group. The cardiomyocytes keep integrity and ordered arrangement, with clear cellular nuclei. There is no inflammatory cells infiltration. *B*: The myocardium from MI-0 d group. The histological observation shows the disordered arrangement of cardiomyocytes, cellular degeneration, necrosis and inflammatory cells infiltration. Scale bar, 50 μm.

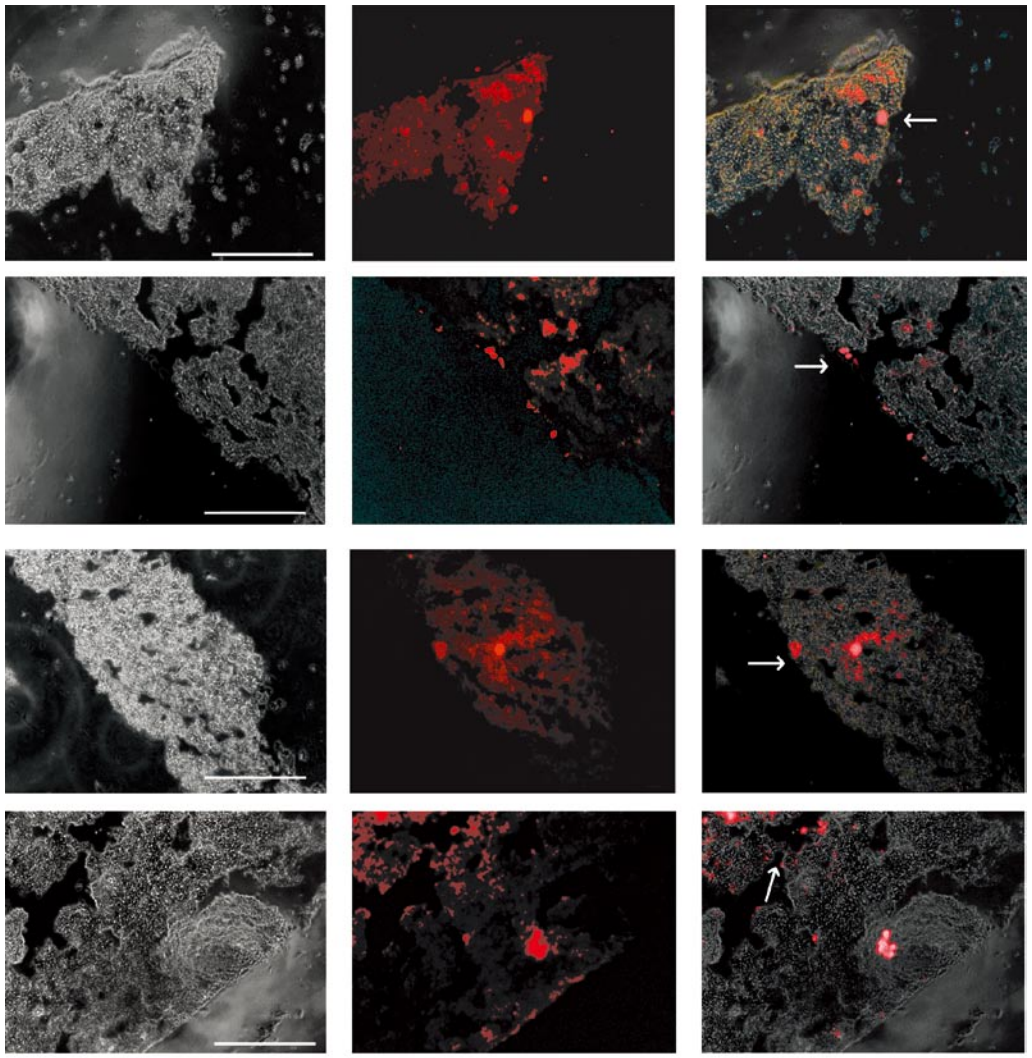

Fig. 2. Morphological location of Nkx2-5^{+} CPCs in mouse bone marrow. Four bone marrow longitudinal sections from different areas are observed under either visible light (left column) or fluorescence fields (middle column). The images of visible light and fluorescence fields are merged in right column. The red fluorescence emitted under 550 nm wave length indicates that the sporadically distributed Nkx2-5^{+} CPCs reside in bone marrow niche (middle column).White arrows indicate that BM-derived Nkx2-5^{+} CPCs locate close to the blood sinus inside cavitas medullaris. Scale bar, 40 μm.

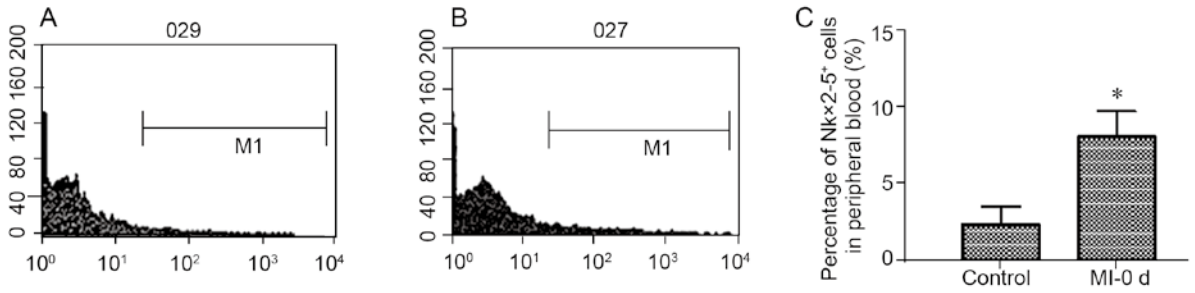

Fig. 3. Flow cytometry analysis of the BM-derived Nkx2-5$^+$ CPCs quantity in peripheral blood. The flow cytometry graphs illustrated the percentages of BM-derived Nkx2-5$^+$ CPCs in peripheral blood mononuclear cells in the control (*A*) and MI-0 d groups (*B*). Statistic analysis (*C*) indicated that the percentage of Nkx2-5$^+$ CPCs in MI-0 d group was significantly higher than that in control group. mean±SD, n=3. $^*P$<0.01 *vs* control.

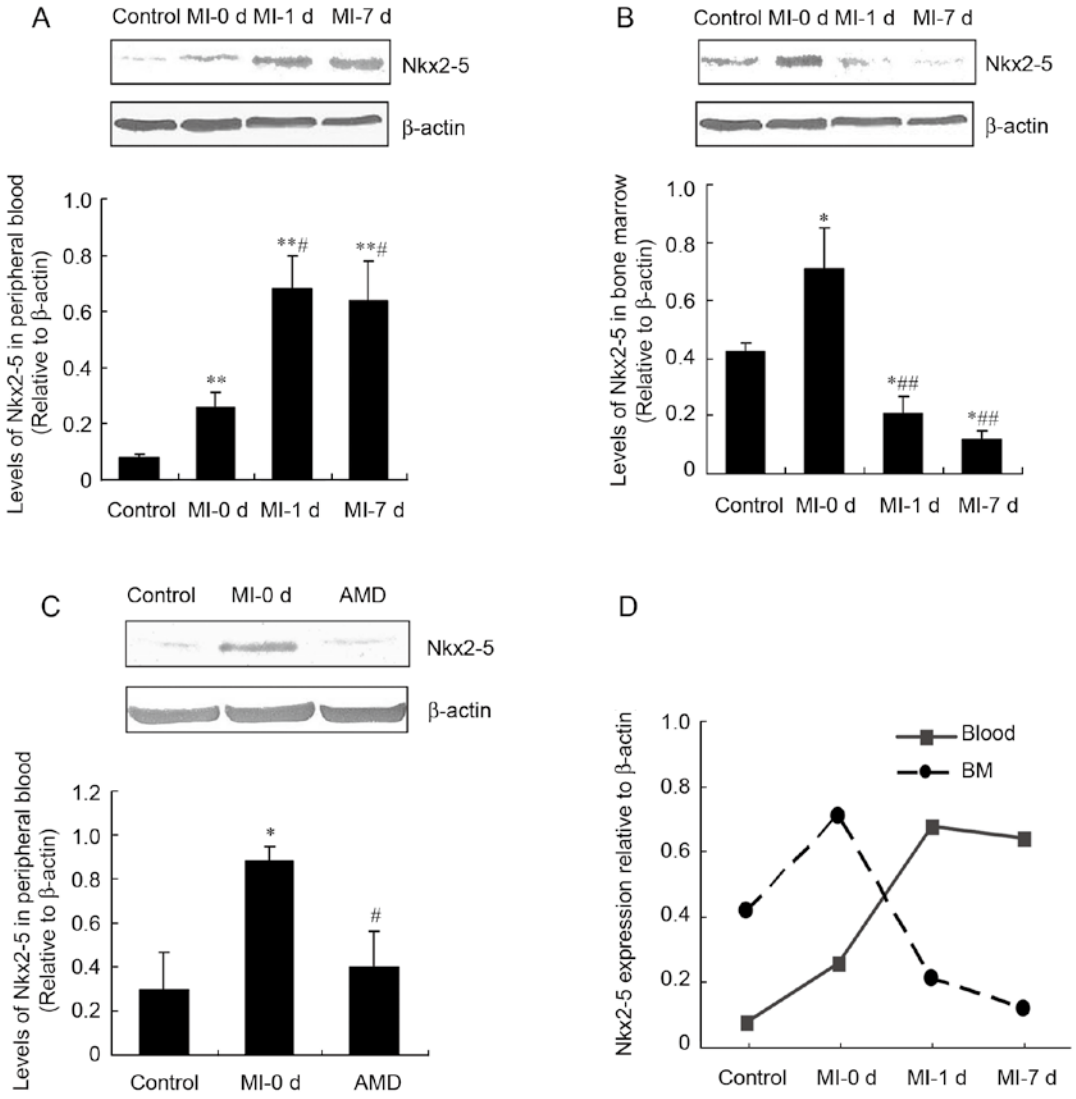

Fig. 4. Western blot results of the levels of Nkx2-5 protein expression. Expressions of Nkx2-5 protein in peripheral blood and bone marrow are shown in *A* and *B*, respectively. The effects of AMD3100 pretreatment on the expression of Nkx2-5 protein in peripheral blood are present in *C* . mean±SD, n=6. $^*P$<0.05, $^*P$<0.01 *vs* control group, $^{\#}P$<0.05, $^{\#\#}P$<0.01 *vs* MI-0 d group. The change curves of Nkx2-5 protein in peripheral blood and bone marrow are illustrated in *D*.

and remained stable until 7 d post-AMI, whereas in BM (dashed line), upregulated expression of Nkx2-5 protein after initiation of AMI rapidly reversed to a lower level by the end of 7-day AMI.

2.6 Expressions of Nkx2-5 protein in peripheral blood in different organ ischemia conditions

With regard to the tissue ischemia in different organs, the level of Nkx2-5 protein expression in MI-0 d group was significantly higher than those in control, limb and cerebral ischemia groups (P<0.01). There was no statistical significance among the control, limb and cerebral ischemia groups (Fig. 5).

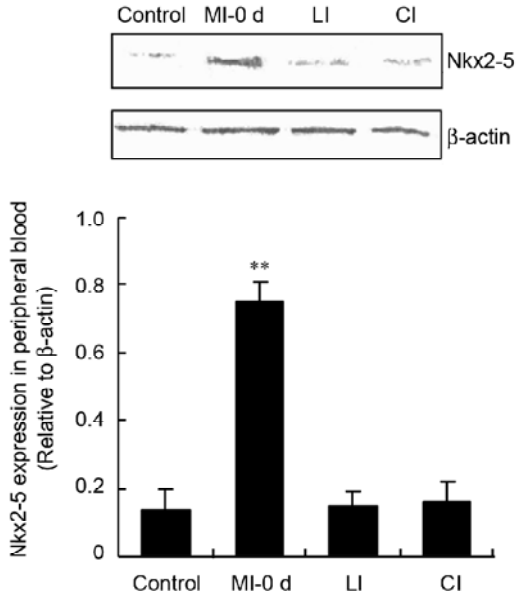

Fig. 5. Expressions of Nkx2-5 protein in peripheral blood in response to different organs ischemia. The level of Nkx2-5 protein expression in MI-0 d group was significantly higher than those in control, limb and cerebral ischemic groups. mean±SD, n=6. $^{**}P$<0.01 *vs* other three groups. There is no significant difference in Nkx2-5 protein expression among control, limb and cerebral ischemia groups.

3 DISCUSSION

Recent research has reported that BM was considered as a source of circulating CXCR4$^+$/CD45$^-$ TCSCs[15]. TCSCs contain mRNA of early skeletal muscle (Myf-5, MyoD, Myogenin), neural (Nestin, GFAP), liver (CK19, α-fetoprotein), intestinal epithelium (Tcf4, CDX1, Msi1h) or cardiac muscle (Nkx2-5, GATA-4, MEF-2C) markers. TCSCs populations maintain the regenerative capacity of terminally differentiated organs, both under physiological condition and following local tissue impairment[16].

In our experiment, we found a morphological evidence of Nkx2-5$^+$ CPCs residing in BM niche without any primary inducement, and these cells showed immature cardiac cells phenotype. Interestingly, BM-derived Nkx2-5$^+$ CPCs were localized in the blood sinusoid of cavitas medullaris physiologically. This phenomenon perhaps explains why BM-derived Nkx2-5$^+$ CPCs are easily mobilized to enter peripheral blood under the pathological stimulation of myocardial ischemia.

Nkx2-5, also known as Csx, is an evolutionarily conserved cardiac transcription factor, and is required for embryonic heart development. While in postnatal period, Nkx2-5 is unavailable in organs except the heart[1]. With Transwell culture apparatus, Kucia *et al*. [15], at cell level, found that BM stem cells expressing early cardiac marker (Nkx2-5) were strongly chemoattracted and migrated to the environment where the supernatant extracted from infarcted myocardium was added. But whether BM-derived Nkx2-5$^+$ CPCs can be mobilized especially in response to AMI *in vivo* remains unclear. In our study, we found that the Nkx2-5 protein expression in peripheral blood was rapidly upregulated, peaked at 24 h, and then remained steady without further enhancement to 7 d following extended period of AMI. With regard to BM, the expression of Nkx2-5 protein increased remarkably at 24 h after AMI rather than decreased. Following consecutive AMI, Nkx2-5 protein expression in BM decreased from 48 h to 7 d after AMI. Our results indicated that AMI induced the changes of Nkx2-5 protein expressions both in blood and BM *in vivo*, and this phenomenon also revealed that AMI initiated a special mobilization of BM-derived Nkx2-5$^+$ CPCs.

As for the reasons why the expression of Nkx2-5 protein in BM was increased early after AMI, altered environment was likely to induce BM-derived stem/progenitor, MSCs for instance, to transform to Nkx2-5$^+$ CPCs. Kucia *et al*. [17] had identified a type of special cells population deposited in BM, which presented the embryonic-like stem cells phenotype and expressed CXCR4/ SSEA-1/Oct-4. These cells could transdifferentiate to CPCs under the culture with special media derived from heart. Based on the data above, we considered that these small embryonic-like stem cells may contribute to replenishing BM-derived Nkx2-5$^+$ CPCs and increasing the content of CPCs and Nkx2-5 protein expression in response to the altered environment in BM early after AMI. But, after all, the capacity of the special embryonic-like stem cells replenishment was limited, besides, BM-derived MSCs proliferation and transdifferentiation alone were also inadequate to rapidly reconstitute BM-derived

Nkx2-5$^+$ CPCs pools to the baseline level. Therefore, the level of Nkx2-5 protein expression in BM was in continuous decrease after peaked mobilization.

To date, the detailed mechanisms of BM-derived stem/progenitor mobilization remain unclear. The reports from other investigators had shown that the mobilization of BM progenitors *in vivo* involved certain complicated processes triggered by key molecules such as adhesion molecule, chemotatic factor or growth factors, and these molecules mediated those processes timely and orderly[18, 19]. It has been generally recognized that stromal derived factor 1 (SDF-1), a potent chemoattractant for CXCR4$^+$ cells, and its receptor CXCR4 (a seven-transmembrane, G-protein-coupled receptor), expressed both on HSCs and TCSCs[20,21]. SDF-1 can exert an adhesive function by binding CXCR4-expressing TCSCs to the position of ischemic tissue. Some data also indicate that SDF-1 is markedly upregulated in the myocardium under tissue ischemia and SDF-1/CXCR-4 axis is required for trafficking progenitor cells from BM to peripheral blood, and homing, engrafting and retaining them in target organ during tissue ischemia[22,23]. Abbott *et al*.[24] transferred SDF-1 into the ischemia heart by adenoviral gene delivery, which doubled BM MSCs recruitment 48 h after MI, but did not enhance recruitment in the absence of MI. In our result, we detected that pretreatment with AMD3100, an SDF-1/CXCR4 antagonist, inhibited the mobilization of BM-derived Nkx2-5$^+$ CPCs during AMI when compared with that in AMI alone, indicating that SDF-1/CXCR4 axis contributed to mobilization of BM-derived Nkx2-5$^+$ CPCs under AMI circumstance.

Experimentally, in order to avoid the influences of surgical stress and inflammatory reaction on mobilization of Nkx2-5$^+$ CPCs, we employed ISO, a stimulant for β-receptor, to induce myocardial ischemia in the manner of a non-invasive procedure[25-27]. ISO has both chronotropic and inotropic activities, which lead to tachycardia and enhance ventricular contraction significantly. ISO also increases myocardial oxygen demand, whereas higher ventricular end-diastolic pressure may decrease blood flow to endocardium, resulting in severe ischemia and hypoxia in myocardium. With high dose of ISO, our histologic results had shown the pathological alterations of myocardial ischemia. Prior studies showed that the limb, brain or heart ischemia may initiate the mobilization of BM-derived endothelial progenitor cells (EPCs) and improve post-ischemia angiogenesis[28,29]. Pathologically, since the different kinds of organ ischemia are able to induce the BM-derived EPCs mobilization, angiogenesis, as a tissue regenerative behavior, it has no organ specificity. With regard to BM-derived CPCs expressing Nkx2-5, whether these cells can be mobilized in the same situations is unknown so far. In present study, we found that BM-derived Nkx2-5$^+$ CPCs mobilization responded sensitively to AMI only, but did not appear at the settings of hind-limb and cerebral ischemia, which demonstrated that the mobilization of BM-derived Nkx2-5$^+$ CPCs possessed predominant organ-specificity.

In conclusion, we proved that Nkx2-5$^+$ CPCs located in BM and also revealed the change of Nkx2-5 protein expression both in blood and BM after AMI, suggesting AMI specially initiated the mobilization of BM-derived Nkx2-5$^+$ CPCs and SDF-1 played a critical role in a chemoattractant manner in the process of mobilization. Nevertheless, our study is the preliminary investigation of BM-derived Nkx2-5$^+$ CPCs mobilization in response to AMI *in vivo*, the morphological evidence that mobilized BM-derived Nkx2-5$^+$ CPCs colonize in ischemia myocardium after AMI and the detailed mechanisms of BM-derived Nkx2-5$^+$ CPCs participating in endogenous cardiomyocyte regeneration need to be further elucidated.

REFERENCES

1 Orlic D, Kajstura J, Chimenti S, Anderson SM, Li B, Pickel J, Mckay R, Nadal-Ginard B, Bodine DM, Leri A, Anversa P. Bone marrow cells regenerate infarcted myocardium. Nature 2004; 410; 701-705.

2 Pittenger MF, Martin BJ. Mesenchymal stem cells and their potential as cardiac therapeutics. Circ Res 2004; 95: 9-20.

3 Kudo M, Wang Y, Wani MA, Xu M, Ayub A, Ashraf M. Implantation of bone marrow stem cells reduces the infarction and fibrosis in ischemic mouse heart. J Mol Cell Cardiol 2003; 35: 1113-1119.

4 Xiao YF. Cardiac application of embryonic stem cells. Acta Physiol Sin (生理学报) 2003; 55(5): 493-504.

5 Zhang DZ (张瑞珍), Gai LY, Liu HW. Differences between adipose-derived stem cells and mesenchymal stem cells in differentiation into cardiomyocytes. Acta Physiol Sin (生理学报) 2008; 60(3): 341-347 (Chinese, English abstract).

6 Dimmeler S, Zeiher AM, Schneider MD. Unchain my heart: the scientific foundations of cardiac repair. J Clin Invest 2005; 115: 572-583.

7 Yoon YS, Park JS, Tkebuchava T, Luedeman C, Losordo DW. Unexpected severe calcification after transplantation of bone marrow cells in acute myocardial infarction. Circulation 2004; 109(25): 3154-3157.

8 Kucia M, Ratajczak J, Ratajczak MZ. Bone marrow as a source of circulating CXCR4$^+$ tissue-committed stem cells. Biol Cell 2005; 97: 133-146.

9 Deb A, Wang S, Skelding KA, Miller D, Simper D, Caplice NM. Bone marrow-derived cardiomyocytes are present in adult human heart: A study of gender-mismatched bone marrow transplantation patients. Circulation 2003; 107(9): 1247-1249.

10 Mouquet F, Pfister O, Jain M, Oikonomopoulos A, Ngoy S, Summer R, Fine A, Liao R. Restoration of cardiac progenitor cells after myocardial infarction by self-proliferation and selective homing of bone marrow-derived stem cells. Circ Res 2005; 97(11): 1090-1092.

11 Kofidis T, Bruin JL, Yamane T. Balsam LB, Lebl DR, Swijnenburg RJ, Tanaka M, Weissman IL, Robbins RC. Insulin-like growth factor promotes engraftment, differentiation, and functional improvement after transfer of embryonic stem cells for myocardial restoration. Stem Cells 2004; 22: 1239-1245.

12 Horsburgh K, McCulloch J, Nilsen M, McCracken E, Large C, Roses, A D, Nicoll JA. Intraventricular infusion of apolipoprotein E ameliorates acute neuronal damage after global cerebral ischemia in mice. J Cereb Blood Flow Metab 2000; 20: 458-462.

13 Yamamoto Y, Wang B, Fukuhara S , Ikehara S, Good RA. Mixed peripheral blood stem cell transplantation for autoimmune disease in BXSB/MpJ mice. Blood, 2002; 100(5): 1886-1893.

14 Yu HL (于红丽), Xu ZW, Zhang ZM, Dong HY. Nanogold-sliver enhancement technique for location of Nkx2.5 cells in bone marrow niche. Acta Acade Med Xuzhou (徐州医学院学报) 2006; 26: 296-298 (Chinese, English abstract).

15 Kucia M, Dawn B, Hunt G, Guo Y, Wysoczynski M, Majka M, Ratajczak J, Rezzoug F, Ildstad ST, Bolli R, Ratajczak MZ. Cell expressing early cardiac markers reside in the bone marrow and are mobilized into the peripheral blood after myocardial infarction. Circ Res 2004; 95: 1191-1199.

16 Kereiakes DJ. Stem cells: the chameleon of the youth. Circulation 2003; 107: 929-934.

17 Kucia M, Reca R, Campbell FR, Zuba-Surma E, Majka M, Ratajczak J, Ratajczak MZ. A population of very small embryonic-like (VSEL) CXCR4t-SSEA-1tOct-4t stems cells identified in adult bone marrow. Leukemia 2006; 20: 857-869.

18 Thomas J, Liu F, Link DC. Mechanisms of mobilization of hematopoietic progenitors with granulocyte colony-stimulating factor. Curr Opinion Hematol 2002; 9: 183-189.

19 Heeschen C, Aicher A, Lehmann R, Fichtlscherer S, Vasa M, Urbich C, Mildner-Rihm C, Martin H, Zeiher AM, Dimmeler S. Erythropoietin is a potent physiologic stimulus for endothelial progenitor cell mobilization. Blood 2003; 102: 1340-1346.

20 Iwaguro H , Yamaguchi J , Kalka C , Murasawa S, Masuda H, Hayashi S, Silver M, Li T, Isner JM, Asahara T. Endothelial progenitor cell vascular endothelial growth factor gene transfer for vascular regeneration. Circulation 2002; 105: 732-738.

21 Kucia M, Wojakowski W, Reca R, Machalinski B, Gozdzik J, Majka M, Baran J, Ratajczak J, Ratajczak MZ. The migration of bone marrow-derived non- hematopoietic tissue-committed stem cells is regulated in an SDF-1-, HGF-, and LIF-dependent manner. Arch Immunol Ther Exp 2006; 54: 121-135.

22 Ratajczak MZ, Kucia M, Reca R, Majka M, Janowska-Wieczorek A, Ratajczak J. Stem cell plasticity revisited: CXCR4-positive cells expressing mRNA for early muscle, liver and neural cells "hide out" in the bone marrow. Leukemia 2004; 18: 29-40.

23 Ma Q, Jones D, Springer TA. The chemokine receptor CXCR4 is required for the retention of B lineage and granulocytic precursors within the bone marrow microenvironment. Immunity 1999; 10: 463-471.

24 Abbott JD, Huang Y, Liu DG, Hickey R, Diane SK, Frank JG. Stromal cell-derived factor-1 plays a critical role in stem cell recruitment to the heart after myocardial infarction but is not sufficient to induce homing in the absence of injury. Circulation 2004; 110: 3300-3305.

25 Pinelli A, Trivulzio S, Tomasoni L, Brenna S, Bonacina E, Accinn R. Isoproterenol-induced myocardial infarction in rabbits. Protection by propranolol or labetalol: a proposed non-invasive procedure. Eur J Pharm Sci 2004; 23(3): 277-285.

26 Trivedi CJ, Balaraman R, Majithiya JB, Bothara SB. Effect of atorvastatin treatment on isoproterenol-induced myocardial infarction in rats. Pharmacology 2006; 77(1): 25-32.

27 Hasić S, Jadrić R, Kiseljaković E, Mornjaković Z, Winterhalter-Jadrić M. Troponin T and histological characteristics of rat myocardial infarction induced by isoproterenol. Bosn J Basic Med Sci 2007; 7(3): 212-217.

28 Falco DE, Porcelli D, Torella AR, Straino S, Iachininoto MG, Orlandi A, Truffa S, Biglioli P, Napolitano M, Capogrossi MC, Pesce M. SDF-1 involvement in endothelial phenotype and ischemia-induced recruitment of bone marrow progenitor cells. Blood 2004; 104: 3472-3482.

29 Hill WD, Hess DC, Martin-Studdard A, Carothers JJ, Zheng J, Hale D, Maeda M, Fagan SC, Carroll JE, Conway SJ. SDF-1 (CXCL12) is upregulated in the ischemic penumbra following stroke: association with bone marrow cell homing to injury. J Neuropathol Exp Neurol 2004; 63: 84-96.